

See discussions, stats, and author profiles for this publication at: <https://www.researchgate.net/publication/343945452>

# Fluorophore-conjugated *Helicobacter pylori* recombinant membrane protein (HopQ) labels primary colon cancer and metastases in orthotopic mouse models by binding CEA-related cell adh...

Article in *Translational oncology* · August 2020

DOI: 10.1016/j.tranon.2020.100857

CITATIONS

0

READS

56

13 authors, including:



**Verena Schmitt**

University Hospital Essen

8 PUBLICATIONS 21 CITATIONS

SEE PROFILE



**Siamak Amirfakhri**

University of California, San Diego

17 PUBLICATIONS 17 CITATIONS

SEE PROFILE



**Alexej Schmidt**

Umeå University

19 PUBLICATIONS 331 CITATIONS

SEE PROFILE



**Marene IB Landström**

Umeå University

109 PUBLICATIONS 4,373 CITATIONS

SEE PROFILE

Some of the authors of this publication are also working on these related projects:



Ефективність liquid biopsy та тканинної біопсії у діагностиці та лікуванні злоякісних пухлин [View project](#)



Hormones in cancer [View project](#)



## Fluorophore-conjugated *Helicobacter pylori* recombinant membrane protein (HopQ) labels primary colon cancer and metastases in orthotopic mouse models by binding CEA-related cell adhesion molecules

Hannah M. Hollandsworth<sup>a,b,c</sup>, Verena Schmitt<sup>d</sup>, Siamak Amirfakhri<sup>a,b,c</sup>, Filemoni Filemoni<sup>a,b,c</sup>, Alexej Schmidt<sup>e</sup>, Maréne Landström<sup>e</sup>, Mykola Lyndin<sup>f</sup>, Steffen Backert<sup>g</sup>, Markus Gerhard<sup>h</sup>, Gunther Wennemuth<sup>d</sup>, Robert M. Hoffman<sup>a,b,c,i</sup>, Bernhard B. Singer<sup>d,1</sup>, Michael Bouvet<sup>a,b,c,\*,1</sup>

<sup>a</sup> Department of Surgery, University of California, La Jolla, CA, USA

<sup>b</sup> Moores Cancer Center, University of California San Diego, La Jolla, CA, USA

<sup>c</sup> VA San Diego Healthcare System, San Diego, CA, USA

<sup>d</sup> Institute of Anatomy, University Hospital, University Duisburg-Essen, Essen, Germany

<sup>e</sup> Medical Biosciences, Umeå University, Umeå, Sweden

<sup>f</sup> Department of Pathology, Sumy State University, Sumy, Ukraine

<sup>g</sup> Department of Biology, Division of Microbiology, Friedrich Alexander University Erlangen, Erlangen, Germany

<sup>h</sup> Institute for Medical Microbiology, Immunology and Hygiene, Technical University Munich, Munich, Germany

<sup>i</sup> AntiCancer, Inc., San Diego, CA, USA

### ARTICLE INFO

#### Article history:

Received 9 June 2020

Received in revised form 10 August 2020

Accepted 12 August 2020

Available online xxx

#### Abbreviations:

rHopQ

Topic:

recombinant HopQ

CEACAM

Topic:

carcinoembryonic antigen-related cell adhesion molecules

rHopQ-IR800

Topic:

recombinant HopQ conjugated to near-infrared

IRDye800CW

TBR

Topic:

tumor to background ratio

### ABSTRACT

HopQ is an outer-membrane protein of *Helicobacter pylori* that binds to human carcinoembryonic antigen-related cell-adhesion molecules (CEACAMs) with high specificity. We aimed to investigate fluorescence targeting of CEACAM-expressing colorectal tumors in patient-derived orthotopic xenograft (PDOX) models with fluorescently labeled recombinant HopQ (rHopQ). Western blotting, flow cytometry and ELISA were performed to determine the efficiency of rHopQ binding to CEACAMs. rHopQ was conjugated to IR800DyeCW (rHopQ-IR800). Nude mice received orthotopic implantation of colon cancer tumors. Three weeks later, mice were administered 25 µg or 50 µg HopQ-IR800 and imaged 24 or 48 h later. Intravital images were analyzed for tumor-to-background ratio (TBR). Flow cytometry and ELISA demonstrated binding of HopQ to CEACAM1, 3 and 5. Dose-response intravital imaging in PDOX models demonstrated optimal results 48 h after administration of 50 µg rHopQ-IR800 (TBR = 3.576) in our protocol. Orthotopic models demonstrated clear tumor margins of primary tumors and small regional metastases with a mean TBR = 3.678 (SD ± 1.027). rHopQ showed specific binding to various CEACAMs in PDOX models. rHopQ may be useful for CEACAM-positive tumor and metastasis detection for pre-surgical diagnosis, intra-operative imaging and fluorescence-guided surgery.

© 2020 The Authors. Published by Elsevier Inc. on behalf of Neoplasia Press, Inc. This is an open access article under the CC BY-NC-ND license (<http://creativecommons.org/licenses/by-nc-nd/4.0/>).

**Abbreviations:** rHopQ, recombinant HopQ; CEACAM, carcinoembryonic antigen-related cell adhesion molecules; rHopQ-IR800, recombinant HopQ conjugated to near-infrared IRDye800CW; TBR, tumor to background ratio.

\* Corresponding author at: UCSD Moores Cancer Center, 3855 Health Sciences Drive #0987, La Jolla, CA 92093-0987, USA.

E-mail address: [mbouvet@ucsd.edu](mailto:mbouvet@ucsd.edu) (M. Bouvet).

<sup>1</sup> Both authors contributed equally to this work.

<http://dx.doi.org/10.1016/j.tranon.2020.100857>

1936-5233/© 2020 The Authors. Published by Elsevier Inc. on behalf of Neoplasia Press, Inc. This is an open access article under the CC BY-NC-ND license (<http://creativecommons.org/licenses/by-nc-nd/4.0/>).

## Introduction

Cancer is a leading cause of human death worldwide with colorectal cancer as the third most common cancer and the fourth highest cause of cancer related mortality, usually due to liver metastasis [1]. Surgical resection is a conventional part of the treatment plan for patients with colorectal cancer. In recent years, there has been a transition in surgical management of colorectal cancer to more minimally invasive techniques, such as laparoscopic and robotic platforms, which leads to a loss of tactile feedback for the surgeon and restricts their field of view.

Despite effective surgical techniques, previous studies have reported a 5.3% rate of radial margin positivity, defined as residual disease at the surgical resection margin [2]. Fluorescence-guided surgery (FGS) can improve the detection of tumor margins and residual positive disease after resection. Prior studies in orthotopic colon cancer mouse models have demonstrated that FGS can improve detection of tumor margins and lead to increased rates of successful disease-free resection [3–5]. Another cause of progression of colon cancer is undetected occult metastases.

Previously, carcinoembryonic antigen (CEA) has been identified as an ideal target for in vivo imaging specifically addressing colorectal tumors [6]. CEA, also named CEACAM5 or CD66e, is a glycosylphosphatidylinositol (GPI)-anchored cell-surface glycoprotein that has been found to be overexpressed in the majority of colorectal cancers [7]. CEA belongs to the carcinoembryonic antigen-related cell-adhesion molecule (CEACAM) family, which is a member of the immunoglobulin superfamily. CEACAMs have been considered as reliable biomarkers and targets for a wide variety of epithelial malignancies, including colorectal cancer [8]. In normal epithelial tissue, most CEACAMs are involved in cell-cell communication and help to modulate various cellular processes [9,10]. In malignant epithelial tissue, CEACAMs may play a role in tumorigenesis and the development of metastases [8].

Recently, it has been shown that *Helicobacter pylori* (*H. pylori*) specifically binds via its outer membrane protein HopQ to human CEACAM1, 3, 5 and 6 [11,12]. The HopQ-CEACAM interaction seemed to be independent of calcium as well as pH and indispensable for the translocation of the oncogenic effector protein CagA into human host cells [13,14].

We have previously demonstrated that CEACAMs are ideal targets for imaging of patient-derived orthotopic xenograft (PDOX) nude mouse models using an anti-CEACAM antibody conjugated to a near infrared fluorophore [15]. In the present study, we utilized the fluorescence-labeled recombinant bacterial protein HopQ to test its suitability for fluorescence targeting of colorectal tumors in PDOX and orthotopic colon cancer cell-line models.

## Materials and methods

### Antibodies and reagents

Cell-culture media and media supplements were purchased from Gibco-Life Technology (Eggenstein, Germany) and the chemicals were obtained from Sigma (Taufkirchen, Germany), unless stated differently. Hybridoma secreting the mouse monoclonal antibody (mAb) 6G5j (specific for human CEACAM1/3/5/6/8) have been recently described [15]. The anti His 2B6 and isotype matched IgG controls were purchased from LeukoCom (Germany) and c-Myc tag specific mAb 9E10 was purchased from AbD Serotec (Germany). Fluorescein isothiocyanate (FITC), phycoerythrin (PE) and horseradish peroxidase (HRP)-coupled secondary goat anti-mouse IgG F(ab)2 fragments, streptavidin-Cy3 and streptavidin-PE were obtained from Jackson ImmunoResearch (West Grove, PA).

### Recombinant HopQ production

The HopQ gene fragment, encoding amino acids 22 to 447, was amplified using genomic DNA prepared from *H. pylori* strain P12 (Qiagen DNeasy Blood and Tissue Kit, Hilden, Germany), Taq Platinum polymerase (Invitrogen, USA) and oligonucleotides that incorporated the restriction site *Nco*I in the

sense (5'-gaatagggccatggcggaagaacaacggcgttttttaagcgt-3') and BamHI in the and antisense (5'-acgtatggatccagggtgttccaagtcttgaataag-3') primer. The column-purified PCR-product was digested with *Nco*I and BamHI, gel-purified, and cloned into the appropriately digested plasmid pOPE101 (Genbank #Y14585). The expression cassette consists of a pelB leader, the truncated HopQ22-447 sequence which is followed by c-Myc- and a (His)<sub>6</sub>-tag sequence.

The plasmid was transformed into *E. coli* XL10 Gold (Stratagene, USA) and transformants were selected for on LB agar plates containing 100 µg/ml carbenicillin, 12.5 µg/ml tetracycline and 0.1 M glucose as a repressor. For expression, an overnight culture in selective LB medium (100 µg/ml carbenicillin, 12.5 µg/ml tetracycline and 0.1 M glucose) was diluted in freshly prepared analogous selective medium and grown at 37 °C until an optical density (at 600 nm) of 0.6 was reached, after which protein expression was induced by the addition of IPTG to a final concentration of 75 µM. After 12 h induction at 24 °C (230 rpm), the proteins were harvested from the periplasmic space as described [16]. Briefly, the pelleted bacteria were resuspended in 1/16 culture volume of cold spheroblast solution (50 mM Tris-HCl pH = 8.0, 20% sucrose, 1 mM EDTA) and gently shaken for 1 h at 4 °C. The suspension was centrifuged at 30,000 g for 1 h at 4 °C and the supernatant, representing the periplasmic extract, was dialyzed twice overnight against 5 l of PBS at 4 °C. The solution was passed through a 0.45 µm filter and adjusted to 0.5 M NaCl and 20 mM imidazole for loading on a Ni-NTA FPLC-column (GE-Healthcare, USA). The (His)<sub>6</sub>-tagged protein was eluted with elution buffer (PBS adjusted to 0.5 M NaCl and 0.5 M imidazole). Protein-containing fractions were dialyzed twice overnight against 2 l of PBS at 4 °C. rHopQ aliquots were adjusted to 1 mg/ml with PBS and stored at –80 °C. Purity and integrity of the protein was confirmed by Coomassie-gel staining and immunoblot using the c-Myc tag specific mAb 9E10. The expected molecular weight of the processed rHopQ is 47.8 kDa, including the tags.

### Cell culture

The epithelial cell lines LS174T (human colon carcinoma), MKN45 (gastric carcinoma), HT29, Caco-2 (colon carcinoma) and A549 (lung carcinoma) cancer cell lines (American Type Culture Collection, Manassas, VA) all endogenously expressing CEACAM1, CEACAM5 and CEACAM6 were cultured in DMEM (GIBCO) supplemented with 10% (v/v) heat inactivated fetal calf serum (FCS) and 4 mM L-glutamine at 37 °C in a humidified atmosphere with 5% CO<sub>2</sub>. For the experiments in the present study, cells were used at tight confluency due to highest CEACAM expression as previously shown [17]. Chinese-hamster ovary (CHO) transfectants were cultured in DMEM (GIBCO, USA) supplemented with 1 mg/ml G418, 10% (v/v) heat inactivated FCS and 4 mM L-glutamine. In all cases, cell viability was tested before use and found to be over 90% as measured by trypan blue exclusion.

### Fluorophore conjugation

Coupling of rHopQ to phycoerythrin (PE) was performed with the lightning-link rapid PE labeling kit (Expedeon/Abcam, Berlin, Germany), to DL488 using the Lightning-Link® Rapid DyLight 488 Antibody Labeling Kit (Novus Biological), to biotin with the Mix-n-Stain biotin antibody labeling kit (Sigma) and for IR800 with the IR800DyeCW (IR800) NHS ester system (LI-COR Biosciences Inc., Lincoln, NE) according to the manufacturer's protocol. rHopQ-IR800 was incubated on a rotator plate (Fisher Scientific, Hampton, NH) under basic conditions at room temperature for 2 h. Gel desalting columns (Thermo Fisher Scientific, Waltham, MA) were used for removal of unbound dye by adding the mixture and centrifuging three times at 2115 g for 3 min. After centrifugation, the rHopQ-IR800 flow-through was removed from the column and stored at 4 °C until further use.

### Direct enzyme-linked immunosorbent assay (ELISA)

Direct ELISA was performed with indicated cell lysates dispensed at 100 µl per well in 96-well microplates (Nunc MaxiSorp) in triplicates. After

blocking with 360  $\mu$ l 1% bovine-serum albumin/phosphate-buffered saline (BSA/PBS), wells were incubated with 100  $\mu$ l of 5  $\mu$ g/ml rHopQ diluted in 1% BSA/PBS, washed 3 times with PBS and labeled with 100  $\mu$ l anti-His mAb 2B6 (5  $\mu$ g/ml). Control staining samples were incubated with mAb 6G5j or isotype matched control (5  $\mu$ g/ml). Wells were then washed three times with PBS and incubated with horse-radise peroxidase (HRP)-coupled goat anti-mouse antibody (Jackson ImmunoResearch Lab Inc., West Grove, PA). After washing, staining was developed with 100  $\mu$ l/well tetramethylbenzidine solution (TMB Xtra, EcoTrak). The enzymatic reaction was stopped with 200 mM H<sub>2</sub>SO<sub>4</sub> solution and absorbance was measured at 450 nm in a microtiter plate reader (Sunrise, Tecan).

#### Flow cytometry

Indicated cell types were labeled with rHopQ-DL488 (10  $\mu$ g/ml in 1,25 dilution) or mAb 6G5j (10  $\mu$ g/ml) diluted in 3% FCS/DMEM for 1 h, washed with 3% FCS/DMEM. For the mAb - labeling incubation was with FITC conjugated goat anti-mouse F(ab')<sub>2</sub> antibody (Jackson ImmunoResearch Lab Inc., West Grove, PA) diluted 1:50 in 3% FCS/DMEM. Background fluorescence was determined using isotype matched Ig. The stained cell samples were analyzed in a FACScalibur flow cytometer (Becton Dickinson, Franklin Lakes, NJ) and the data were processed utilizing CellQuest software (Becton Dickinson, Franklin Lakes, NJ). Where applicable, dead cells, identified by PI staining (5  $\mu$ g/ml), were excluded from the determination.

To determine the dose-response of rHopQ, rHopQ-biotin and rHopQ-PE we incubated 100,000 CHO-CEACAM1 cells were incubated with 5, 10 and 20  $\mu$ g/ml of rHopQ, rHopQ-biotin and rHopQ-PE, respectively. Subsequently, the rHopQ-biotin was labeled with Streptavidin-PE, the rHopQ with anti His mAb 2B6 (10  $\mu$ g/ml) followed by goat anti mouse pAb-PE (1,50). Samples were analyzed in a FACScalibur flow cytometer (Becton Dickinson).

#### Immunofluorescence (IF)

Serial sections of 4  $\mu$ m were prepared from 4% paraffin-embedded human jejunum tissues, previously fixed in neutrally buffered formalin, mounted on 3-aminopropyltriethoxysilane-coated slides and were then demasked, by incubation for 10 min at 95 °C in citrate buffer pH 6. Endogenous peroxidase activity was blocked by treatment with 3% H<sub>2</sub>O<sub>2</sub> for 5 min and subsequent washing with PBS. HT29 cells grown on cover slips were fixed similarly. Cells on cover slips and tissue sections were then blocked with 1% BSA/PBS and stained with 10  $\mu$ g/ml rHopQ-biotin followed either by Cy-3- (IF) coupled streptavidin (Jackson ImmunoResearch Lab Inc., West Grove, PA). The samples were washed after each staining step with cold PBS three times. HRP-staining was developed with 3,3-diaminobenzidine (DAB, brown precipitate) and the reaction was stopped by several washes with PBS. Stained tissue sections were mounted and documented by microscopy. Fluorescence staining was analyzed with the Leica DMI4000B microscope.

#### Western blotting

Indicated cell-lines were lysed in RIPA-based lysis buffer containing 50 mM Tris-HCl, pH 7.5, 150 mM NaCl, 1% Triton X-100, 0.5% sodium deoxycholate supplemented with protease inhibitor cocktail set III (Calbiochem, San Diego, CA) and PhosSTOP phosphatase inhibitor cocktail (Roche, Basel Switzerland) and incubated on ice for 30 min. Lysates were centrifuged at 10,000g and 4 °C for 15 min. Approximately 50  $\mu$ g of total protein was subjected to SDS-PAGE, blotted onto nitrocellulose membranes (Schleicher & Schuell, Dassel, Germany) and reacted with 10  $\mu$ g/ml mAb 6G5j (positive control), 10  $\mu$ g/ml isotype control mAb and 10  $\mu$ g/ml rHopQ followed by anti-His mAb 2B6, respectively. After washing, HRP-coupled goat anti mouse pAb was added and subsequently detected with an ECL chemiluminescence substrate and monitored by the LAS3000 gel documentation system (Fuji, USA). The loading control with  $\beta$ -actin was detected by HRP-coupled mouse anti  $\beta$ -actin according to the manufacturer's protocol (Sigma Aldrich, A3854).

#### Binding kinetics (IC<sub>50</sub>)

To determine the binding kinetics of anti-CEACAM antibody 6G5j compared to rHopQ, recombinant CCl1-Fc or CCl1-V-Fc comprising the entire extracellular domain, or only the variable region respectively of human CEACAM1, were expressed as human IgG1 Fc-fusion proteins in 293 HEK cells. Purified proteins were coated on a Nunc ELISA plate (Maxisorp, #439454, ThermoScientific, USA) at 500 ng/well (over-night at 4 °C in 0.1 M Na<sub>2</sub>CO<sub>3</sub> buffer pH 9.6) and blocked with 2% Milk-PBS (1 h at RT). Serial dilutions of the 6G5j antibody or the HopQ protein were incubated over-night at 4 °C. Bound antibody was detected with an HRP-conjugated polyclonal goat anti-mouse antibody (DAKO,P0447) whereas the bound HopQ was detected with a biotinylated anti-myc antibody (#9E10, AbD Serotec, for 2 h at RT), followed by HRP-conjugated Streptavidin (Roche Diagnostics GmbH, REF 11089153001, 30 min at RT). The TMB-color formation was blocked by addition of H<sub>2</sub>SO<sub>4</sub> (after approximately 30 s), and absorbance measured at 450 nm. The ELISA plate was washed three times with T-PBS after each incubation step. For calculation of the IC<sub>50</sub>, the concentration sufficient to obtain 50% saturation, the maximum and minimal values were set to 100 and 0% respectively and a non-linear regression was modelled (Prism 7, GraphPad, USA). The option "inhibitor versus normalized response" with a variable slope was chosen for the IC50 calculation.

#### Animals

Female and male nude mice (nu/nu) age 4–6 weeks were purchased from The Jackson Laboratory (Bar Harbor, ME). Mice were housed in a bio-safety room and fed an autoclaved standard mouse diet. For surgical procedures, mice were anesthetized with an intraperitoneal injection of xylazine, ketamine and PBS. Post-procedural pain was treated with subcutaneous buprenorphine. At the conclusion of the experiments, mice were euthanized by CO<sub>2</sub> inhalation followed by cervical dislocation. Studies were approved by the San Diego Veterans Administration Medical Center Institutional Animal Care and Use Committee (IACUC, animal use protocol A17-020).

#### Establishment of subcutaneous colon cancer cell-line tumors in nude mice

Nude mice ( $n = 2$ ) were administered inhaled isoflurane and the flank was prepped with 70% ethanol solution. Under sterile conditions, LS174T cells ( $1 \times 10^6$ , American Type Culture Collection, Manassas, VA) reconstituted in 50  $\mu$ L Matrigel Matrix (Corning Life Sciences, Corning, NY) and 50  $\mu$ L cold PBS were injected into the bilateral flanks subcutaneously. Tumors grew until they were approximately 5 mm in diameter in nude mice. Tumors were resected and divided into 1 mm fragments for subsequent orthotopic implantation, as described below.

#### Establishment of colon cancer orthotopic models

Patient-derived tumors were chosen based on previously published data demonstrating over-expression of CEACAM in C4 and Lung 4 tumor lysates (C4 = surgically-resected patient primary colon cancer and Lung 4 = surgically resected colon cancer lung metastasis) [15]. Lung 4 and C4 cell-lines represent patient-derived colon tumors obtained at our institution under IRB protocol 140,046 with informed patient consent and established in nude mice as transplantable tumors.

For orthotopic implantation, nude mice ( $n = 11$ ) were administered intraperitoneal ketamine cocktail to induce anesthesia. The abdomen was sterilized with a 70% ethanol solution. A small incision was made in the midline through the skin and peritoneum. The cecum was carefully identified. A 2 mm fragment of tumor, previously grown subcutaneously in nude mouse models was implanted onto the serosa of the cecum using an 8–0 nylon suture (Ethicon Inc., Sommerville, NJ). Four mice received orthotopic implantation of a Lung 4 tumor fragment to determine appropriate dose and time of imaging, as described below. Six mice received

orthotopic implantation of LS174T tumor fragments to establish models as described below. One mouse received orthotopic implantation of a C4 tumor fragment, to confirm efficacy in PDOX mouse models. The peritoneum and skin were closed with a 6-0 nylon suture (Ethicon Inc., Sommerville, NJ). Tumors grew until palpable, or approximately 5 mm in diameter [18,19].

### Fluorescence imaging

Once tumor growth was sufficient as defined, Lung 4 PDOX mice ( $n = 4$ ) were administered 25  $\mu\text{g}$  or 50  $\mu\text{g}$ , respectively, of rHopQ-IR800, reconstituted in PBS, via tail vein injection. Mice were imaged 24 or 48 h after administration. Prior to imaging, mice were administered intraperitoneal anesthesia and the cecum was surgically exposed. Imaging was performed on the LI-COR Pearl Trilogy Small Animal Imaging System (LI-COR, Lincoln, NE), which is equipped for fluorescent imaging at 700 and 800 nm. Once an appropriate dose and time of imaging was determined, orthotopic cell-line models ( $n = 6$ ), and an additional C4 PDOX models were imaged 48 h after administration of 50  $\mu\text{g}$  of rHopQ-IR800 reconstituted in PBS via tail vein injection, in order to confirm that these conditions could brightly visualize the tumor.

### Statistical analysis

The tumor to background ratio (TBR) was calculated as the maximum tumor fluorescence signal divided by maximum background fluorescent signal under the conditions used. Background was set as the surrounding intra-abdominal organs, mainly small bowel. Fluorescence signals were quantified with automated areas generated with the Image Studio Software, with a consistent standard deviation from background signal of 10 and minimum of 250 pixels per area. Mean TBR was calculated for mice imaged 48 h after administration of 50  $\mu\text{g}$  of rHopQ-IR800 using SPSS version 24 (IBM, Armonk, NY).

## Results

Flow cytometric analyses using CHO-cell transfectants expressing either human CEACAM 1, 3, 4, 5, 6, 7 and 8 demonstrated binding of rHopQ-PE to CEACAM 1, 3 and 5 (Fig. 1a). Isotype matched IgG and 6G5j as CEACAM binding monoclonal antibody (mAb) were used as negative and positive controls, respectively. rHopQ binding to human CEACAM 1, 3 and 5 was confirmed by ELISA. Indicated CHO transfectant lysates were immobilized and detected by rHopQ followed by anti-His mAb 2B6 detection or mAb 6G5j staining as positive control (Fig. 1b). Western blotting demonstrated that rHopQ detected endogenously expressed CEACAM1 with a molecular weight of approximately 120 kDa and CEACAM5 with a molecular weight of approximately 180 kDa in lysates of epithelial cell lines derived from gastric (MKN45), colon (HT29, Caco-2) and alveolar (A549) cancer cell lines (Fig. 2). Additionally, rHopQ bound to lysates of CHO cells expressing CEACAM1 and 5 (Fig. 2a).

Next, we analyzed the performance of rHopQ-PE by immunohistochemical staining (IHS) utilizing 4% PFA fixed HT29 cells (Fig. 2c) and sections of human jejunal tissue (Fig. 2d) and rHopQ-PE binding was similar to previous findings using anti-CEACAM antibody 6G5j [15]. In order to estimate the affinity of rHopQ against CEACAM1, we determined the IC<sub>50</sub> against two eukaryotically expressed CEACAM1-Fc fusion proteins, as indicated by the concentration resulting in 50% maximal binding. The IC<sub>50</sub> of HopQ against the CEACAM1-Fc fusion protein containing the full-length extracellular domain or the V-region only was 2.5 and 1.7 nM respectively. This high affinity is found to be in the same range as obtained for the positive control antibody 6G5j (2.3 and 2.4 nM, respectively) that had been previously used for tumor detection (Fig. 3) [15].

Dose-response intravital imaging of colon cancer PDOX models ( $n = 4$ ) of Lung 4 after administration of 25  $\mu\text{g}$  rHopQ-IR800 demonstrated a low TBR 24 and 48 h after administration (TBR = 0.901 and 1.220, respectively) (Fig. 4a, b). After administration of 50  $\mu\text{g}$  rHopQ-IR800, PDOX models of Lung 4 imaged 24 h later had a TBR = 1.781 (Fig. 4c). 48 h

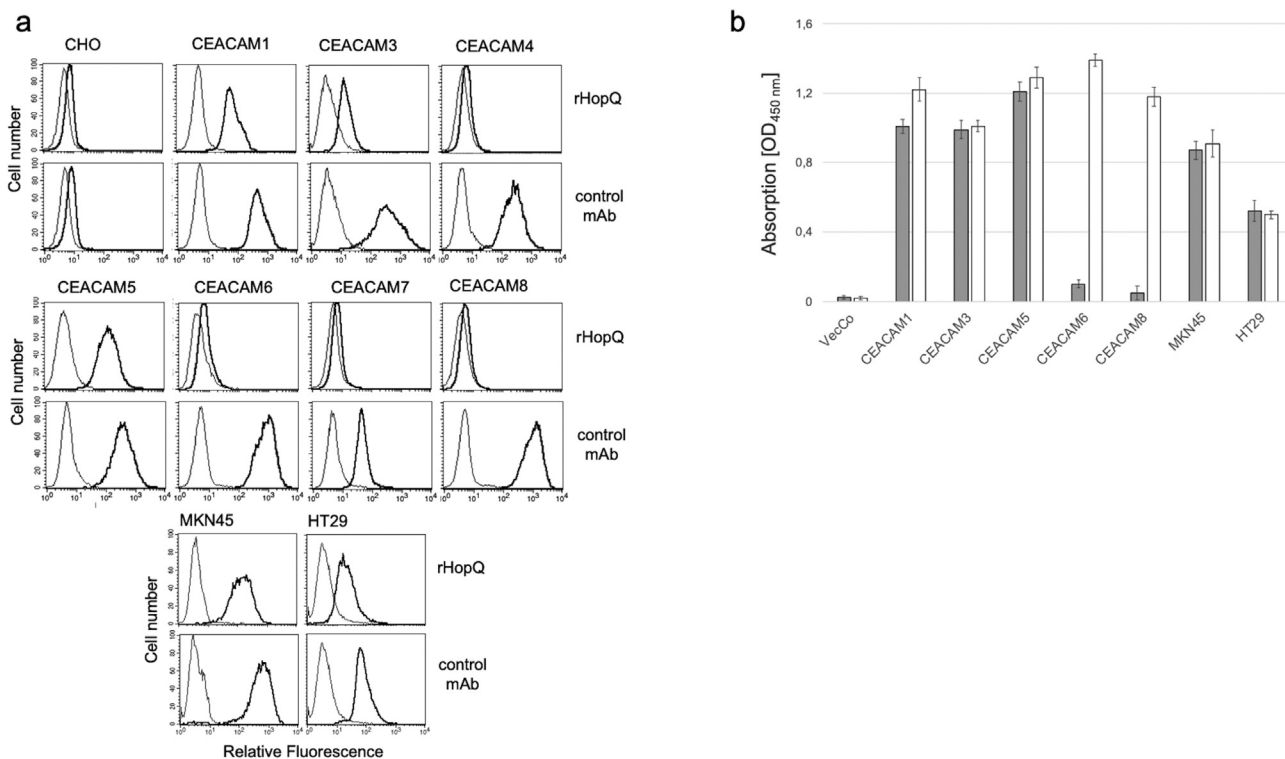


**Fig. 1.** Recombinant HopQ binding properties. (a) Flow cytometric analyses of rHopQ-PE binding to CHO transfectants expressing indicated human CEACAMs and endogenously CEACAM-expressing cell-lines. rHopQ and positive control mAb staining are shown with a black line, negative control staining is shown with a grey line. (b) ELISA analyzed lysates were immobilized and bound to rHopQ followed by mouse anti-His mAb 2B6 (LeukoCom, Germany, grey bars) or positive control mAb staining (white bars), followed by incubation with HRP-coupled secondary antibody and TMB substrate for staining. Data are representative of three independent experiments.

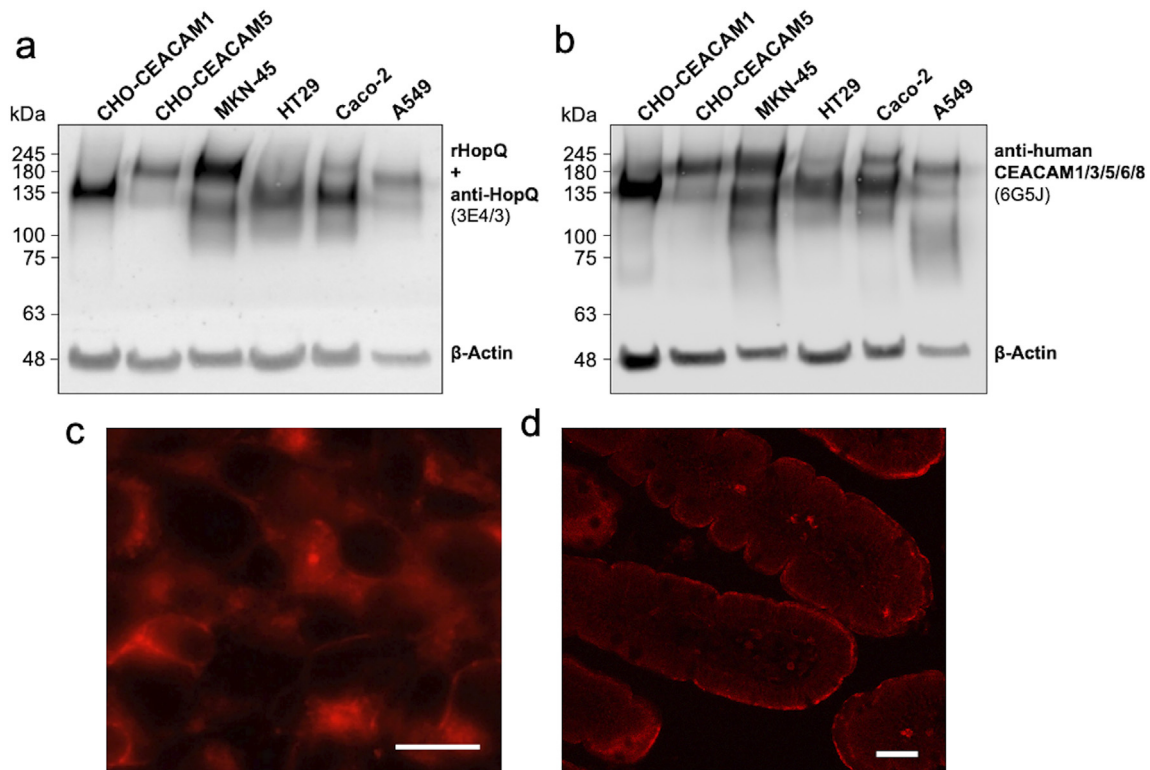


**Fig. 2.** Western blotting, fluorescence staining and immunohistochemistry of recombinant HopQ binding to CEACAM1, CEACAM5, and endogenously expressed CEACAMs. (a) Western blot analysis of the rHopQ (A) and mAb 6G5j (b) binding to lysates originated from CHO-CEACAM1, CHO-CEACAM5, gastric (MKN45), colon (HT29, Caco-2) and alveolar (A549) cancer cell lines as detected by chemiluminescence. Beta actin staining was utilized to control proper loading of samples. Representative data from two separate experiments are shown. (c) Fluorescence staining of paraffin-embedded HT29 cells labeled with 10  $\mu$ g/ml HopQ-PE. (d) Immunohistochemistry of paraffin-embedded human jejunum tissue labeled with 10  $\mu$ g/ml of biotinylated HopQ followed by Cy3-coupled streptavidin. Scale bars represent 100  $\mu$ m.

after administration of 50  $\mu$ g rHopQ-IR800, imaging demonstrated a TBR = 3.576, the highest TBR observed (Fig. 4d). Small tumors < 2 mm in diameter, otherwise invisible, were readily imaged with minimal background signal (Fig. 4c). Visualization was confirmed with another colon cancer PDOX model (C4) with TBR = 3.977, 48 h after administration of 50  $\mu$ g rHopQ-IR800 (Fig. 5).

Orthotopic colon cancer cell-line models ( $n = 6$ ) were imaged 48 h after administration of 50  $\mu$ g rHopQ-IR800. Tumor margins were distinctly identified with a mean TBR = 3.678 (SD  $\pm$  1.027). The LS174T orthotopic colon cancer cell-line model developed regional metastases that measured approximately 2 mm in diameter, which were also distinctly viewed with fluorescence imaging, which were otherwise invisible (Fig. 6).

## Discussion

For the first time, we show in the present report that a bacterial adhesion protein can potentially be utilized for detecting metastatic colorectal cancer in a clinically relevant PDOX mouse model. Recombinant HopQ-IR800 specifically binds to CEACAM1 and 5 for near-infrared fluorescence visualization of orthotopic cell-line and PDOX mouse models of colon cancer. The results of the present study are consistent with our previous findings that CEACAMs are ideal targets for in vivo fluorescence imaging of colon cancer, as demonstrated in our PDOX mouse models with an anti-CEACAM antibody-fluorophore conjugate [15]. Important to note, rHopQ binds to CEACAM1 [13] even when coupled with diverse fluorochromes

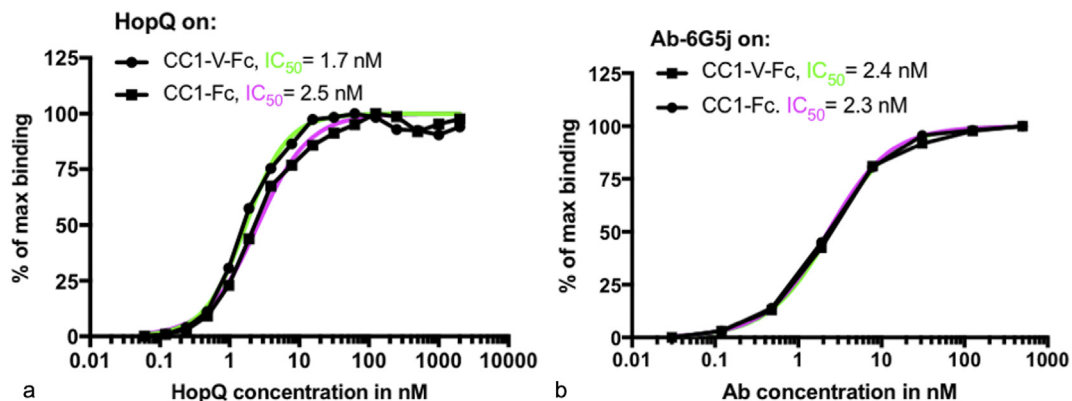


**Fig. 3.** Recombinant HopQ protein (a) or the antibody 6G5j (b) were incubated in serial dilutions on ELISA-plate coated with CC1-Fc and CC1-V-Fc respectively. The concentration sufficient to obtain half-maximum binding ( $IC_{50}$ ) was calculated by usage of a non-linear regression fit. The HopQ demonstrated an  $IC_{50}$  of 2.5 nM against the CC1-Fc and 1.7 nM against the CC1-V-Fc protein respectively (a). Likewise, the 6G5j antibody showed an almost identical  $IC_{50}$  of 2.4 (2.3) nM against both proteins (b). The non-linear regression curves are depicted in color.

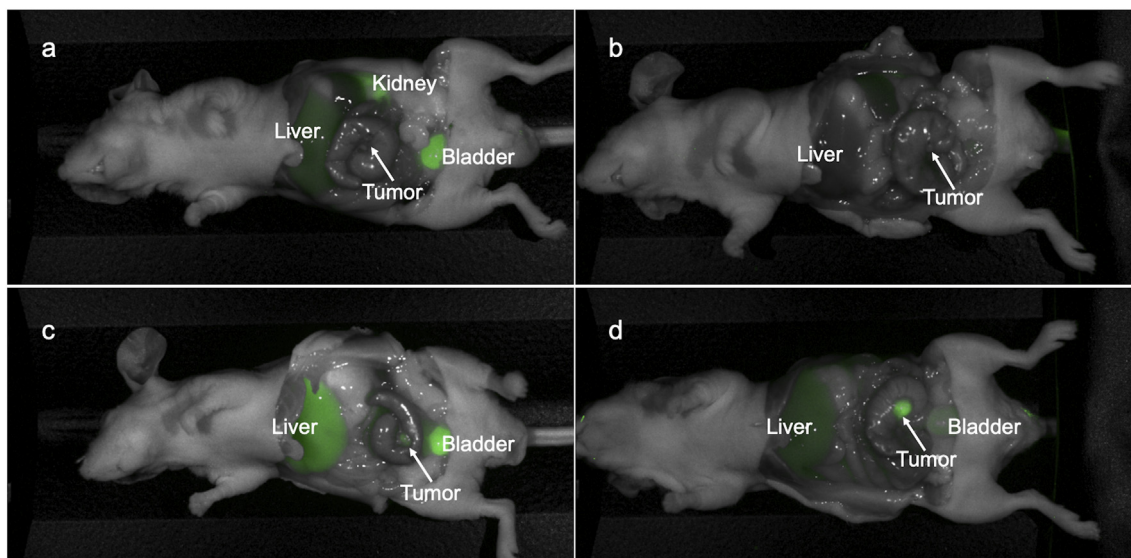


**Fig. 4.** Dose-response fluorescence imaging of the Lung 4 PDOX model demonstrates distinct tumor margins of tumors <2 mm in diameter. (a) Imaged 24 h after administration of 25 µg rHopQ-IR800, TBR = 0.901. (b) Imaged 48 h after administration of 25 µg rHopQ-IR800, TBR = 1.220. (c) Imaged 24 h after administration of 50 µg rHopQ-IR800, TBR = 1.781. (d) Imaged 48 h after administration of 50 µg rHopQ-IR800, TBR = 3.576.

or biotin. Therefore, rHopQ can be used for a wide variety of applications including flow cytometry, ELISA, western blotting and immunohistochemical approaches. Of the conditions tested, imaging at 48 h gave the best tumor-to-background ratio. In contrast to glycosylated antibodies, rHopQ is a bacterial protein without glycosylation protecting it from degradation. Although rHopQ has been demonstrated in previous literature to bind CEACAM1, 3, 5 and 6 [11,12], we were puzzled that we did not observe CEACAM6 interaction. However, it may be that HopQ has a higher affinity to CEACAM1, 3 and 5 whereas the interaction with CEACAM6 has low affinity. Further analyses need to be done to clarify this hypothesis.

CEACAMs have been demonstrated to be a useful target for fluorescence-guided surgery. While anti-CEACAM antibody 6G5j-IR800 has been demonstrated to have a TBR of 3.17 [15], in the present study we found that rHop-IR800 has a mean TBR of 3.678. When compared to previously published data on anti-CEACAM antibody 6G5j [15], which has a molecular weight of 150 kDa, rHopQ has a molecular weight of 47 kDa, which may allow rHopQ to be more efficiently delivered to its target than the larger antibody. Future studies will be performed to directly compare the properties of 6G5j-IR800 and rHopQ-IR800 in orthotopic mouse models of colon cancer.

Previously, it has been shown that fluorescence-guided surgery (FGS) is effective for achieving complete tumor resection and decreasing tumor

recurrence rates in orthotopic mouse models [3,4]. The present study demonstrates that rHopQ-IR800 was able to detect small primary tumors and metastases, which is promising for possible effective FGS. Further studies are needed to confirm this hypothesis. In addition to primary colon cancer, fluorescence imaging may be useful for imaging of colorectal metastases. Small hepatic metastases are often difficult to identify on pre-operative imaging or with intra-operative imaging and can significantly worsen prognosis [20]. A previous study demonstrated that fluorescence imaging can improve detection and resection of colon cancer-derived hepatic metastases [21,22]. The present study shows that rHopQ-IR800 is effective for imaging of occult colorectal cancer metastases.

In the present study, orthotopic colon cancer cell-line tumors and two colon cancer PDOX models, one from a primary patient tumor and the other from a metastatic tumor, were fluorescently visualized with rHopQ-IR800, which is promising for successful transition into the heterogeneous clinical setting. The present study emphasizes the importance of orthotopic mouse models in providing clinically relevant models of cancer.

Limitations of this study include a small sample size of mouse models. Further studies will be performed with additional liver metastases models to confirm the efficacy of rHopQ-IR800 at identifying hepatic metastases in a PDOX mouse model. The new book, “Strategies for Curative Fluorescence-Guided Surgery,” edited by Hoffman and Bouvet [23] defines

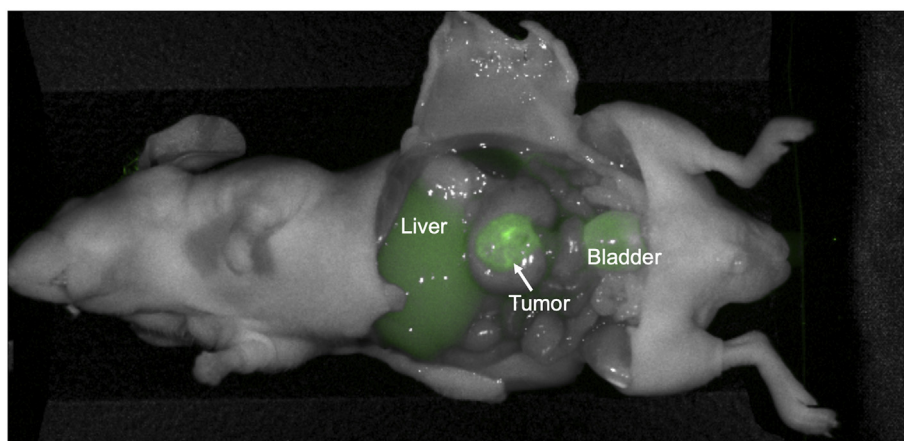


**Fig. 5.** Fluorescence imaging of the C4 PDOX model 48 h after administration of 50 µg rHopQ-IR800, TBR = 3.977.

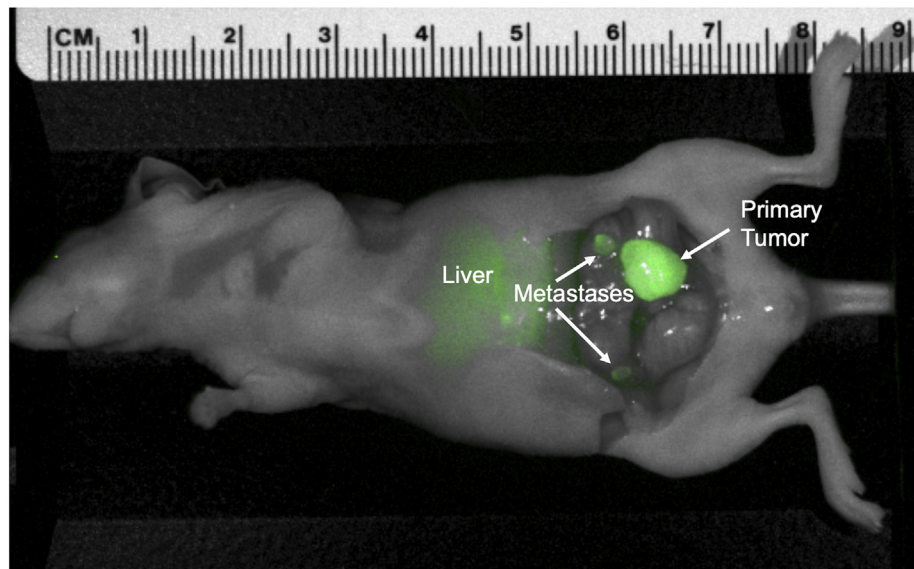


**Fig. 6.** Representative image of orthotopic colon cancer cell-line (LS174T) model, 48 h after administration of 50 µg rHopQ-IR800. Primary tumor and regional metastases margins are distinctly viewed. Mean TBR = 3.678 (SD ± 1.027),  $n = 6$ .

numerous fluorescent probes that were demonstrated to clearly define tumor borders in various mouse models of cancer as well as in the clinic. To date, there are eight antibody-fluorescent probes in clinical development for various cancer types and one protein based fluorescent probe in clinical development [24]. Prior to translation in the clinic, rHopQ-IR800 will require safety and efficacy testing in human cancer patients. Another limitation to this study is that rHopQ is targeted to human tumors, not murine tissues, which can result in artificially elevated TBR. In addition, the ability of rHopQ to bind to multiple CEACAMs may lead to binding of normal tissue in addition to tumor, which may lead to lower TBR. Further studies need to be performed to assess the efficacy of rHopQ to visualize primary and metastatic human colon cancer.

The present study demonstrates high affinity binding of rHopQ to epithelial cancers overexpressing CEACAM, including colon, gastric and lung cancer. Recombinant HopQ enabled fluorescence imaging provides a distinct tumor margins of primary tumors and metastases in PDOX and orthotopic cell-line mouse models of colon cancer. rHopQ may be a useful alternative to CEACAM-specific antibodies for pre-surgical diagnosis, intra-operative imaging and fluorescence-guided surgery (FGS) in epithelial malignancies that overexpress various CEACAMs. The potential advantages of rHopQ over antibody-based imaging probes include lower molecular weight which may lead to improved delivery of the fluorescent probe. Future studies will determine the clinical potential of rHopQ.

#### Funding

This study was funded by VA Merit Review grant numbers 1 I01 BX003856-01A1 and 1 I01 BX004494-01 (MB), NIH/NCI T32CA121938 (HH), and Deutsche Forschungsgemeinschaft DFG Grant SI-1558/3-1 (BS). This work was in part supported by grants from the Swedish Medical Research Council (K2019-01598) and the Swedish Cancer Society to ML.

#### CRediT authorship contribution statement

**Hannah M. Hollandsworth:** Conceptualization, Methodology, Validation, Formal analysis, Resources, Data curation, Visualization, Writing - original draft, Writing - review & editing. **Verena Schmitt:** Conceptualization, Methodology, Validation, Formal analysis, Resources, Data curation, Writing - review & editing. **Siamak Amirfakhri:** Conceptualization, Methodology, Formal analysis, Resources, Data curation, Writing - review & editing. **Filemoni Filemoni:** Methodology, Data curation, Writing - review

& editing. **Alexej Schmidt:** Conceptualization, Methodology, Validation, Formal analysis, Resources, Data curation, Writing - review & editing. **Maréne Landström:** Conceptualization, Methodology, Validation, Formal analysis, Resources, Data curation, Writing - review & editing. **Mykola Lyndin:** Conceptualization, Methodology, Validation, Formal analysis, Resources, Data curation, Writing - review & editing. **Steffen Backert:** Conceptualization, Methodology, Validation, Formal analysis, Resources, Data curation, Writing - review & editing. **Markus Gerhard:** Conceptualization, Methodology, Validation, Formal analysis, Resources, Data curation, Writing - review & editing. **Gunther Wennemuth:** Conceptualization, Methodology, Writing - review & editing, Supervision. **Robert M. Hoffman:** Conceptualization, Writing - review & editing, Supervision. **Bernhard B. Singer:** Conceptualization, Methodology, Validation, Formal analysis, Resources, Data curation, Writing - original draft, Writing - review & editing, Visualization, Supervision. **Michael Bouvet:** Conceptualization, Methodology, Resources, Writing - review & editing, Supervision.

#### Declaration of competing interest

Dr. Hoffman is a non-salaried affiliate of AntiCancer Inc., which used PDOX models for contract research. All other authors have no conflicts of interest to disclose.

#### Acknowledgments

The authors thank Birgit Maranca-Hüwel and Bärbel Gobs-Hevelke for excellent technical support.

#### References

- [1] M. Arnold, M.S. Sierra, M. Laversanne, I. Soerjomataram, A. Jemal, F. Bray, Global patterns and trends in colorectal cancer incidence and mortality, *Gut*. 66 (4) (2017) 683–691, <https://doi.org/10.1136/gutjnl-2015-310912>.
- [2] R. Amri, L.G. Bordeianou, P. Sylla, D.L. Berger, Association of radial margin positivity with colon cancer, *JAMA Surg.* 150 (9) (2015) 890–898, <https://doi.org/10.1001/jamasurg.2015.1525>.
- [3] C.A. Metildi, S. Kaushal, C.S. Snyder, et al., Fluorescence-guided surgery of human colon cancer increases complete resection resulting in cures in an orthotopic nude mouse model, *J. Surg. Res.* 179 (1) (2013) 87–93, <https://doi.org/10.1016/j.jss.2012.08.052>.
- [4] Y. Hiroshima, A. Maawy, C.A. Metildi, et al., Successful fluorescence-guided surgery on human colon cancer patient-derived orthotopic xenograft mouse models using a fluorophore-conjugated anti-CEA antibody and a portable imaging system, *J Lap & Advan Surg Tech.* 24 (4) (2014) 241–247, <https://doi.org/10.1089/lap.2013.0418>.



- [5] C.A. Metildi, S. Kaushal, G.A. Luiken, et al., Fluorescently labeled chimeric anti-CEA antibody improves detection and resection of human colon cancer in a patient-derived orthotopic xenograft (PDOX) nude mouse model, *J. Surg. Oncol.* 109 (5) (2014) 451–458, <https://doi.org/10.1002/jso.23507>.
- [6] J.P. Tiernan, S.L. Perry, E.T. Verghese, et al., Carcinoembryonic antigen is the preferred biomarker for *in vivo* colorectal cancer targeting, *Br. J. Cancer* 108 (2013) 662–667.
- [7] S. Hammarstrom, The carcinoembryonic antigen (CEA) family: structures, suggested functions and expression in normal and malignant tissues, *Semin. Cancer Biol.* 9 (1999) 67–81.
- [8] Nicole Beauchemin, Arabzadeh Azadeh, Carcinoembryonic antigen-related cell adhesion molecules (CEACAMs) in cancer progression and metastasis, *Cancer and Met Reviews.* 32 (2013) 643–671.
- [9] I. Helfrich, B.B. Singer, Size matters: the functional role of the CEACAM1 isoform signature and its impact for NK cell-mediated killing in melanoma, *Cancers (Basel)* 13 (3) (2019) 11.
- [10] K. Kuespert, S. Pils, C.R. Hauck, CEACAMs: their role in physiology and pathophysiology, *Curr. Opin. Cell Biol.* 18 (2006) 565–571, <https://doi.org/10.1016/j.ceb.2006.08.008>.
- [11] A. Javaheri, T. Kruse, K. Moonens, R. Mejias-Luque, A. Debraekeleer, C.I. Asche, et al., *Helicobacter pylori* adhesin HopQ engages in a virulence-enhancing interaction with human CEACAMs, *Nat. Microbiol.* 2 (2016) 16189, (nmicrobiol2016189[pil]) <https://doi.org/10.1038/nmicrobiol.2016.189>.
- [12] V. Königer, L. Holsten, U. Harrison, et al., *Helicobacter pylori* exploits human CEACAMs via HopQ for adherence and translocation of CagA, *Nat. Microbiol.* 2 (2016) 16233, <https://doi.org/10.1038/nmicrobiol.2016.233>.
- [13] K. Moonens, Y. Hamway, M. Neddermann, et al., *Helicobacter pylori* adhesin HopQ disrupts trans dimerization in human CEACAMs, *EMBO.* 37 (13) (2018) 2.
- [14] N. Tegtmeyer, A. Harrer, V. Schmitt, B.B. Singer, S. Backert, Expression of CEACAM1 or CEACAM5 in AZ-521 cells restores the type IV secretion deficiency for translocation of CagA by *Helicobacter pylori*, *Cell. Microbiol.* 21 (1) (2019) e12965.
- [15] H.M. Hollandsworth, S. Amirfakhri, F. Filemoni, et al., Anti-carcinoembryonic antigen-related cell adhesion molecule antibody for fluorescence visualization of primary colon cancer and metastases in patient-derived orthotopic xenograft mouse models, *Oncotarget.* 11 (2020) 429–439.
- [16] Y.Y. Fei, A. Schmidt, G. Bylund, D.X. Johansson, S. Henriksson, C. Lebrilla, J.V. Solnick, T. Borén, X.D. Zhu, Use of real-time, label-free analysis in revealing low-affinity binding to blood group antigens by *Helicobacter pylori*, *Anal. Chem.* 83 (16) (2011) 6336–6341.
- [17] B.B. Singer, I. Scheffrahn, R. Kammerer, N. Suttrop, S. Ergun, H. Slevogt, Dereglulation of the CEACAM expression pattern causes undifferentiated cell growth in human lung adenocarcinoma cells, *PLoS One* 5 (1) (2010) e8747.
- [18] R.M. Hoffman, Patient-Derived Mouse Models of Cancer, Humana Press, Springer International Publishing AG, 2017 <https://doi.org/10.1007/978-3-319-57424-0>.
- [19] X.Y. Fu, J.M. Besterman, R.M. Hoffman, Models of human metastatic colon cancer in nude mice orthotopically constructed by using histologically intact patient specimens, *PNAS* 88 (20) (2015) 9345–9349, <https://doi.org/10.1073/pnas.88.20.9345>.
- [20] A. Klint, G. Engholm, H.H. Storm, L. Tryggvadóttir, M. Gislum, T. Hakulinen, Bray F Trends in survival of patients diagnosed with cancer of the digestive organs in the Nordic countries 1964–2003 followed up to the end of 2006, *Acta Oncol.* 49 (5) (2010) 578–607.
- [21] Y. Hiroshima, T.M. Lwin, T. Murakami, et al., Effective fluorescence-guided surgery of liver metastasis using a fluorescent anti-CEA antibody, *J. Surg. Oncol.* 114 (8) (2016) 951–958, <https://doi.org/10.1002/jso.24462>.
- [22] T. Murakami, Y. Hiroshima, Y. Zhang, et al., Improved disease-free survival and overall survival after fluorescence-guided surgery of liver metastases in an orthotopic nude mouse model, *J. Surg. Oncol.* 112 (2015) 119–124, <https://doi.org/10.1002/jso.23986>.
- [23] R. Hoffman, M. Bouvet, Strategies for curative fluorescence-guided surgery of cancer 1st edition, Elsevier 1 (2020) 21–29.
- [24] C.W. Barth, S.L. Gibbs, Fluorescence image-guided surgery – a perspective on contrast agent development, *Proc. SPIE Int. Soc. Opt. Eng.* 11222 (2020) 112220J, <https://doi.org/10.1117/12.2545292>.